

Identifying Merozoite Surface Protein 4 and Merozoite Surface Protein 7 *Plasmodium falciparum* Protein Family Members Specifically Binding to Human Erythrocytes Suggests a New Malarial Parasite-Redundant Survival Mechanism

Yesid Garcia,^{†‡} Alvaro Puentes,^{†‡} Hernando Curtidor,[‡] Gladys Cifuentes,[‡] Claudia Reyes,[‡] Jose Barreto,[‡] Armando Moreno,[‡] and Manuel E. Patarroyo^{*,†,§}

Fundación Instituto de Inmunología de Colombia, Carrera 50 No. 26-00, CP 020304, Bogotá D.C., Colombia, South America, and Universidad Nacional de Colombia Bogotá, Bogotá D.C., Colombia, South America

Received June 28, 2007

Plasmodium falciparum merozoite surface proteins (MSP-1 to -11) have been involved in merozoite interaction with the red blood cell (RBC) surface. Peptides covering complete MSP-4 and MSP-7 amino acid sequences were synthesized and tested in RBC binding assays. One MSP-4 high activity binding peptide (HABP) and five MSP-7 HABPs were found having specific binding to RBC surface. MSP-4 and MSP-7 HABP binding was sensitive to enzymatic treatment; they recognized a 52 kDa erythrocyte membrane protein. MSP-4 HABP had low invasion inhibition, suggesting it might bind to RBCs and also be involved in physiological mechanisms, while MSP-7 HABPs displayed different invasion inhibition activity (83–24%) in *in vitro* tests, suggesting different roles for both proteins during invasion. Structural characteristics found when comparing the MSP-4 HABP with MSP-HABPs displaying epidermal growth factor-like sequences suggested that these redundant MSP-family proteins could be a new parasite strategy for evading host genetic variability and immune pressure.

Introduction

There were areas of high risk malarial transmission in 107 countries by the end of 2004 and some 3200 million people were living in such areas. It has been estimated that 350 to 500 million episodes of clinical malaria occur annually in these areas, most being caused by *Plasmodium falciparum* infection, causing more than three million deaths per year.¹

The release of this parasite's asexual blood-stage form (merozoite) and its replication byproducts during infected red blood cell (iRBC^o) lysis are the main cause of the disease's symptomatology.² Merozoite invasion of RBC is a multistep process including merozoite rolling, attachment, and reorientation to allow its apical pole to come into contact with the RBC surface,^{3,4} followed by junction and parasitophorous vacuole (PV) formation.⁵ It has been demonstrated that the parasite recognizes RBC during the penetration step via receptor–ligand interactions,⁶ which are a critical mechanism in the parasite's invasion of RBC; blocking them is thus of the utmost importance in vaccine development.⁷

Although very little is known about the particular role of any individual protein, it has been shown by transcriptome analysis that most of the eleven merozoite surface proteins (MSPs) identified to date (MSP-1 to -11) are involved in initial merozoite interaction with RBC and their invasion.⁸ Several members of the MSP family have been postulated as being excellent candidates for being included in a multiepitope, antimalarial vaccine based on the above information, added to abundant experimental evidence.^{9–12}

MSP-1 has been the most characterized MSP protein. It is a 195 kDa protein that undergoes a series of proteolytic cleavages,

thereby producing four polypeptides (MSP-1₈₃, MSP-1₃₀, MSP-1₃₈, and MSP-1₄₂) forming a noncovalently bound complex present on the merozoite surface.^{13,14} The MSP-1₄₂ fragment then undergoes a second proteolytic calcium-dependent (Ca⁺⁺) processing,^{15,16} being cleaved into 33 kDa and 19 kDa fragments at the time of merozoite invasion.¹⁴ This last fragment (MSP-1₁₉), containing two EGF-like domains named I and II,¹³ is anchored to the merozoite's membrane via a glycosyl-phosphatidyl-inositol (GPI) tail and is the only MSP-1 fraction carried into the newly infected erythrocyte.¹⁷

An EGF-like domain I was found between residues 1525 and 1573 of the MSP-1 protein and an EGF-like domain II between residues MSP-1 protein 1574 and 1639, corresponding to residues 16–48 and 49–97, respectively, in the 19 kDa MSP-1 fragment.

It has been suggested that MSP-1 EGF-like domains are crucial for parasite invasion, because serum antibodies from malaria-exposed people recognize these two EGF-domains,¹⁸ and reduced malarial morbidity is associated with antibodies against the fragment's N-terminal portion.¹⁹

A novel MSP family protein member, designated merozoite surface protein-4 (MSP-4), was identified and characterized 10 years ago.²⁰

The MSP-4 gene encodes a 272-amino-acid protein, having a calculated 30.4 kDa and 40 kDa observed molecular mass. The protein's N-terminal region is made up of 15 predominantly hydrophobic amino acids, being characteristic of a secretory signal (SS) sequence.²⁰ The MSP-4 C-terminus consists of 19 hydrophobic residues, preceded by three consecutive serine residues. This hydrophobic region's length and position, together with the presence of serine residues, is strongly reminiscent of several *P. falciparum* and *Trypanosoma brucei* surface proteins anchored to the merozoite's membrane via GPI moieties²¹ (Figure 1a).

Another member of the *Plasmodium falciparum* MSP family named (MSP-7) consists of 351 amino acids (41 kDa calculated mass). A putative 27 amino acid N-terminal signal sequence

* To whom correspondence should be addressed. Professor Manuel E. Patarroyo M.D., Carrera 50 #26-00, Bogotá-Colombia. Tel.: +57-1-4815219/3158919. Fax: +57-1-4815269. E-mail: mepatarr@mail.com.

[†] Both contributed equally well as first authors.

[‡] Fundación Instituto de Inmunología de Colombia.

[§] Universidad Nacional de Colombia Bogotá.

^a Abbreviations: MSP, merozoite surface protein; HABP, high activity binding peptide; ¹²⁵I-HABP, ¹²⁵-iodine radiolabeled HABP; HBS, HEPES buffered saline; CD, circular dichroism; RBC, red blood cell.

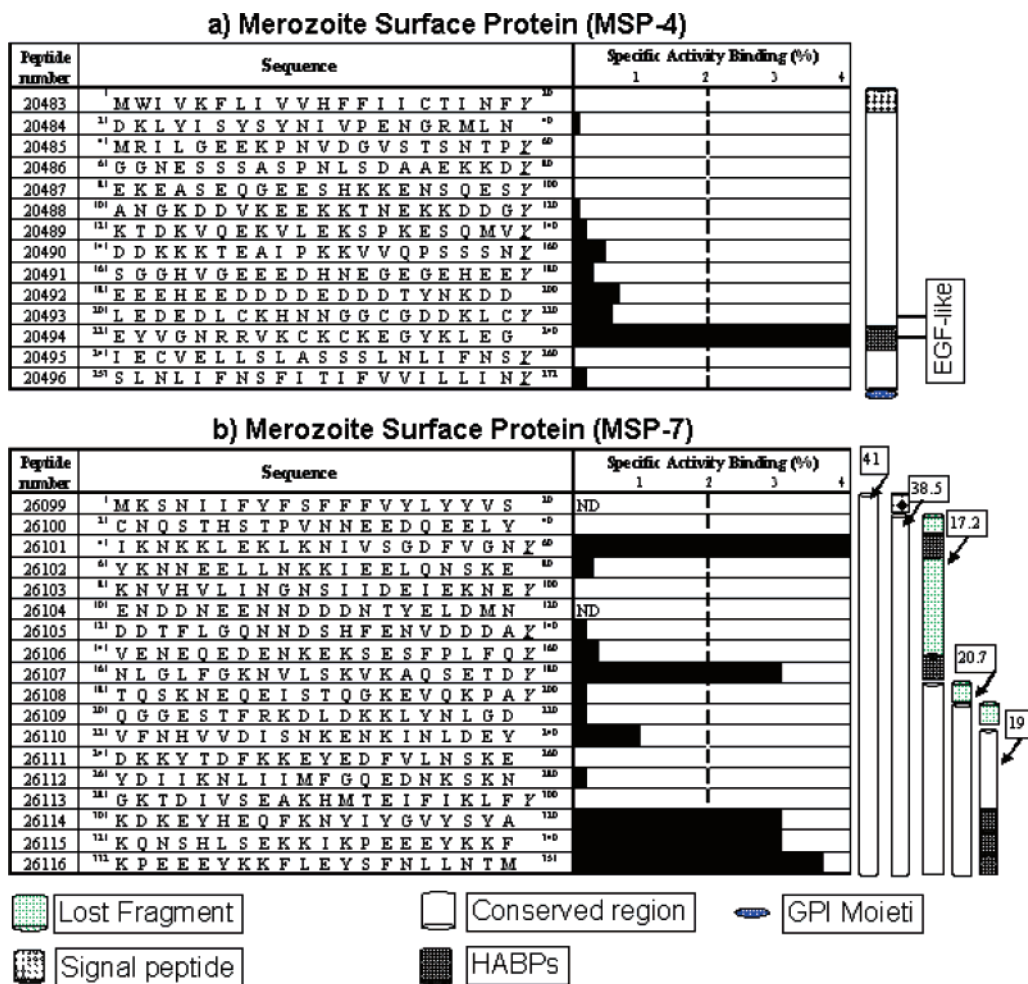


Figure 1. (a) MSP-4 and (b) MSP-7 peptide human erythrocyte binding activity. MSP-4 and MSP-7 synthetic peptide amino acid sequences are shown. Tyrosine residues (underlined and shown in italics) were added at the C-terminus of those peptides, which did not contain it, to be radiolabeled. Peptides having greater than or equal to 2% specific binding activity were considered to be HABPs; all experiments were done in triplicate. The horizontal black bars represent specific binding percentage (slope), and a diagram is presented on the right-hand side showing the molecule, with corresponding domains, anchoring points, and the molecular weight for each cleavage fragment (in kDa) are shown for MSP-7.

(SS) precedes a 324 amino acid (38 kDa) polypeptide.²² The protein is mainly hydrophilic (33% charged residues), having a negative charge cluster from residues 94–148.

Fragments named MSP-7₂₂ and MSP-7₁₉ in the N-terminal region were located at Ser177 and Glu195, respectively, suggesting that the 38.5 kDa precursor undergoes cleavage between residues 176 (Gln) and 177 (Ser) into a 17.2 kDa polypeptide in the N-terminal and another 20.7 kDa one in the C-terminal (20.738, MSP-7₂₂). MSP-7₂₂ is bound to the MSP-1 complex on the merozoite surface and undergoes further cleavage between residues 194 (Gln) and 195 (Glu), removing 18 amino acids from the N-terminus and producing MSP-7₁₉²³ (18.7 kDa; Figure 1b).

The *msp-7* gene is transcribed by mature intracellular asexual blood-stage parasite stages and accumulates at a time coincident with MSP-1 expression. MSP-7 cleavage to produce MSP-7₂₂ probably occurs prior to merozoite release, because the precursor is not detected on the merozoite surface with MSP-7₂₂-specific antibodies.²² MSP-7 has been found to be conserved within the three *P. falciparum* lines examined so far, with only four amino acid substitutions being identified when comparing FCB-1 to 3D7/T9-96 lines.²²

The high degree of sequence homology is in marked contrast with that described for some other MSPs, such as MSP-1, MSP-2, MSP-8, and MSP-10, but similar to that described for MSP-

3, MSP-5, and MSP-6. The fact that the *msp-7* gene is conserved in these parasite lines may suggest that it is not under immune pressure, although sera from donors naturally exposed to malaria do contain antibodies reacting with MSP-7.^{22,23}

In spite of great efforts having been made to find malarial parasite-derived antigens able to induce an effective immune response controlling this disease, a lot of territory still needs to be explored. Our search (using synthetic peptides) has been focused on receptor–ligand interactions that have revealed that many proteins from *Plasmodium falciparum* asexual and hepatic stages appear to be involved in the complex process of human erythrocyte,^{24,25} hepatocyte, and reticulocyte invasion.²⁶

This work describes MSP-4 and MSP-7 synthetic peptides binding to human RBC, which may have a biological implication during such a complex invasion process²⁷ and could be relevant in vaccine development.²⁸

We thus used a highly specific and robust methodology, developed in our Institute, with the specific aim of recognizing high activity binding peptides (HABPs). Only one MSP-4 HABP and five MSP-7 HABPs are reported here, which specifically and saturably bound to normal RBC surface molecules. This binding could be modified when normal erythrocyte surface molecules were enzymatically treated. In vitro invasion inhibition assay results with the HABPs so far identified have suggested an important role for these proteins and their correspond-

ing HABPs in merozoite invasion and, therefore, in the development of a subunit-based, multi-epitope, chemically synthesized, antimalarial vaccine, which is so desperately needed.

Materials and Methods

Peptide Synthesis and Radiolabeling. A total of 14 20-mer peptides covering the complete *P. falciparum* MSP-4 sequence and 18 20-mer peptides covering the complete *P. falciparum* MSP-7 sequence (GenBank accession number AAC32785 and Pf13_0197, respectively) were synthesized by solid-phase multiple peptide system (*t*-Boc strategy) and cleaved by the low-high technique.²⁹ The peptides were lyophilized and purified by reverse-phase high-pressure liquid chromatography and then characterized by MALDI-TOF mass spectrometry. One Tyr residue was added at the C-terminal of those peptides, which did not contain this residue in their native sequences to enable ¹²⁵I-radio-labeling.

Figure 1 shows synthesized sequences in one-letter code. Their position in the protein is in the superscript small numbers on top of the amino acid sequences, and peptide numbers correspond to our Institute's serial number. The radiolabeling was performed according to previously reported assays.^{30,31} In brief, 2 nmol purified peptides were labeled with 5 μ L of Na¹²⁵I (100 μ Ci/mL, ICN) and 0.3 μ mol chloramine-T to a final 20 μ L volume for 15 min; the reaction was stopped with 0.3 μ mol sodium metabisulphite. The ¹²⁵I-radiolabeled peptides were separated on a Sephadex G-10 column (Pharmacia; 80 \times 5 mm) and measured on an automatic gamma counter (Packard Cobra II).

Erythrocyte Binding Assays. The erythrocytes were obtained from human donors in heparinized tubes; the white blood cells were removed, as previously described.^{25,31} Cells were washed five times with HEPES buffered saline (HBS). RBC 2×10^7 cell/ μ L were poured into polystyrene tubes with increasing ¹²⁵I-peptide concentrations (50–300 nM) in the presence or absence of unlabeled peptide (200 excess) and a 200 μ L final volume; they were then incubated for 90 min at room temperature with constant shaking. Cells were then washed twice with 3 mL of HBS; cell-associated radioactivity was quantified on an automatic gamma counter (Packard Cobra II). A total of 14 peptides from the MSP-4 protein and 18 MSP-7 protein peptides were tested in human erythrocyte binding assays. The assays were carried out in triplicate in identical conditions.

The binding assay allowed total binding (cells incubated with just ¹²⁵I-peptide) and nonspecific binding (cells incubated with ¹²⁵I-peptide in the presence of unlabeled peptide) to be determined. The difference between total binding and nonspecific binding represented peptide specific binding.^{26,32} The slope resulting from graphing specific binding represented the ratio between specific bound ¹²⁵I-peptide and added ¹²⁵I-peptide.

Those peptides having binding activity (slope) higher than or equal to 0.02 were considered to be human erythrocyte HABPs (Figure 1), because they had 2% specific RBC binding. Three types of behavior were presented in binding assays, similar to that reported in other studies: peptides which did not bind, nonspecific HABPs (their binding activity was high but they did not present specificity), and specific activity binding peptides (these included low specific binding peptides whose slope was less than 0.02).^{31,33}

Saturation Assays. The saturation binding assay was adapted from previously reported assays.^{25,31} Briefly, RBCs 1.5×10^7 cell/ μ L were incubated with radiolabeled HABPs (¹²⁵I-HABP) at 0 to 1800 nM concentration in the presence or absence of unlabeled peptide (200 excess). An aliquot of supernatant was taken after a 90 min incubation to quantify free ¹²⁵I-HABPs; the cells were then washed twice with 3 mL of HBS. Assays were performed in triplicate and cell-associated radioactivity was measured; aliquots were then used for cross-linking assays (see below). Affinity constant values and the number of binding sites were determined using saturation curves; Hill coefficients were calculated from Hill plot.^{25,31}

Cross-Linking Assay. Aliquots containing 2.5 μ L were taken from MSP-4 HABP 20494 and MSP-7 26114, 26115, and 26116 for human RBC saturation assays and cross-linked with 10 μ M

bis-sulfosuccinimidyl suberate (BS³-Sigma Aldrich) for 30 min at 4 °C. The reaction was stopped with Tris-HCl 25 mM (pH 7.4) for 15 min; cells were then washed thrice with HBS to retire cross-linker excess and free peptide. Samples were then treated with lysis buffer (5% SDS, 10 nM iodoacetamide, 1% Triton X-100, 100 mM EDTA, and 10 mM PMSF). Finally, erythrocyte membranes were pelleted at 15 000 g for 30 min and washed twice with HBS buffer. The pellet was suspended in Laemmli buffer and heated at 90 °C for 2 min. The proteins were separated on 12% SDS-PAGE and were exposed on BioRad Imaging Screen K (BioRad Molecular Imager FX; BioRad Quantity One, Quantitation Software) for 5–8 days. The labeled band's molecular weight was determined by comparison with the apparent standard weight markers low range (Fermentas Life Science).

Human RBC Enzyme Treatment. Human RBC enzyme treatment was modified from the technique described.³¹ Briefly, RBC (1.5×10^7 cell/ μ L, 1 mL final volume) suspended in HBS (pH 7.2) were treated with 150 μ U/mL neuraminidase (ICN 9001–67-6), trypsin (Sigma T-1005), and chymotrypsin (Sigma C-4129) at final 1 mg/mL concentration, 1 h at 37 °C with constant shaking. The samples were then spun at 1000 g for 3 min and washed thrice with HBS. Treated and nontreated erythrocytes were tested in binding assay with HABPs.

Merozoite Invasion Inhibition Assay. Sorbitol-synchronized *P. falciparum* (FCB-2 strain)³⁴ cultures were incubated until late schizont stage at final 0.5% parasitemia and 5% hematocrite in RPMI 1640 + 10% O-positive plasma. Cultures were then seeded in 96-well cell-culture plates (Nunc) in the presence of test peptides at 100 and 200 μ M concentrations. Each peptide was tested in triplicate. Supernatant was recovered after 18 h incubation at 37 °C in 5% O₂, 5% CO₂ and 90% N₂ atmosphere. The human RBC were stained with 15 μ g/mL hydroethidine, incubated at 37 °C for 30 min, and washed thrice with PBS. The suspensions were analyzed by flow cytometry (FACSsort) in Log FL2 data-mode, using CellQuest software (Becton Dickinson immunocytometry system, San Jose, CA).³⁵ Infected and uninfected human erythrocytes and infected human erythrocytes treated with ethylene glycol-bis-(β -aminoethylether-*N,N,N',N'*-tetraacetic acid) (EGTA) and chloroquine were used as controls.

CD Spectroscopy. HABP secondary structure was determined by circular dichroism (CD) spectra and recorded for each HABP at 20 °C on Jasco J-810 spectropolarimeter at wavelengths ranging from 190 to 260 nm in 1.0 cm cuvettes.³⁶ The peptides were dissolved at 0.1 mM concentration in aqueous 30% TFE solution. Each spectrum was obtained from averaging three scans taken at a 20 nm/min scan rate with 1 nm spectra bandwidth, corrected for baseline. The results were expressed as mean residue ellipticity [Θ].

Cross-Competition Assays. The cross-competition assay was done with MSP-4 peptide 20494 *cf* MSP-4 HABP 34668, MSP-8 26373, MSP-10 31132, as well as low-binding MSP-4 20483 peptide used as control. ¹²⁵I-labeled-HABP 20494 (300 nM) was incubated with 1×10^7 cells for 90 min at room temperature in the presence of unlabeled MSP-4 34668, MSP-8 26373, MSP-10 31132, and MSP-4 20483 peptides (3–30 μ M). Cells were washed three times with 3 mL of HBS and cell-bound peptide was quantified, as described above for the binding assay.

Structural Analysis by Molecular Modeling from HABP-20494-MSP4. For the alignments, we use the CLUSTAL method based on first deriving a phylogenetic tree from a matrix of all pairwise sequence similarity scores, obtained using a fast pairwise alignment algorithm. The multiple alignment is then achieved from a series of pairwise alignments of clusters of sequences, following the order of branching in the tree,³⁷ using Geno3D (<http://geno3D-pbil.ibcp.fr>).³⁸

The structural models for MSP-10 (residues 417–498, GenBank accession number AA050199), MSP-8 (residues 495–594, GenBank accession number AF325160), and MSP-4 (residues 213–233, GenBank accession number AAC32785) were calculated by energy minimization strategy using 10 000 steps and 0.001 Å root-mean-square deviation (rmsd), and molecular dynamics was performed with 1 femto second (fs) time step and the length of

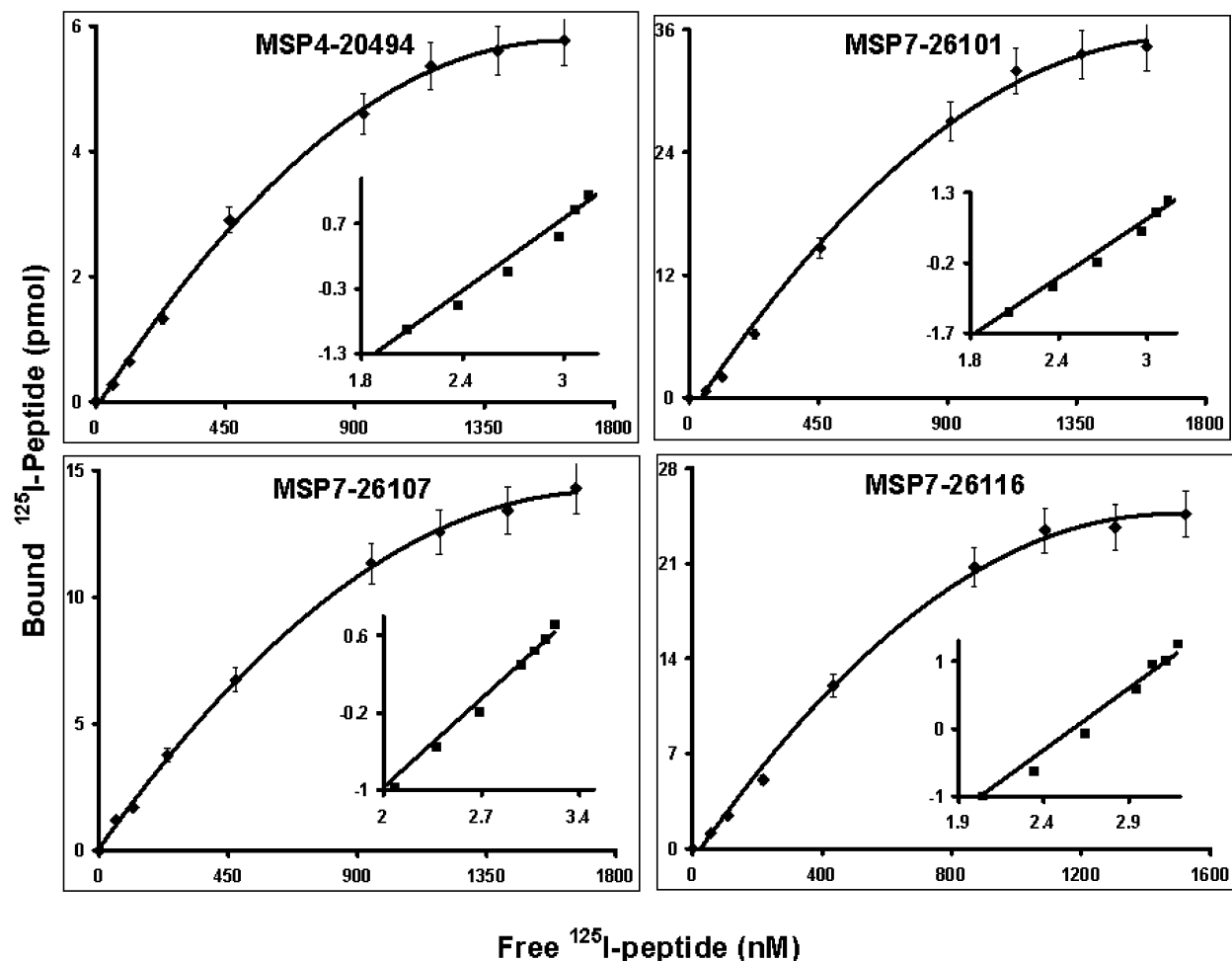


Figure 2. Saturation assays. The saturation curves resulted from graphing specifically bound ¹²⁵I-HABP *cf* free ¹²⁵I-HABP concentration. Affinity constants, as well as maximum number of sites per cell, were obtained from these curves. All experiments were carried out in triplicate. HABP binding was saturable, and the affinity constants were in the nanomolar range. The Hill plot, which determines binding cooperativity between the ligand and the receptor is placed inside the main graph, where the abscissa is log *F* and the ordinate is log(*B*/*B*_{max} - *B*). *B* is pmol bound ¹²⁵I-HABP and *F* is free ¹²⁵I-HABP.

bonds of hydrogen constrains with the SHAKE algorithm. The system was heated to 300 K over 6 pico seconds (ps) using a constant energy with periodic rescaling of molecular velocities, using the Discovery program (Accelrys) for all of them, based on the 3D structure obtained by NMR of the *P. falciparum* MSP-1 19 ka fragment (protein databank ICEJ).³⁹

MSP-4 HABP-34668, MSP-10 HABP-31132,⁴⁰ MSP-8 HABP-26373,³¹ and MSP-1 HABP-5501³² were also localized and structurally compared using Insight II (2000) Biopolymer module software (Accelrys, Inc., Software, U.S.A.) run on an Indigo 2 station (Silicon Graphics). Model quality control was performed using PROCHECK-NMR software.⁴¹

Results

MSP-4 and MSP-7 Peptides Specifically Bound to Human Erythrocytes. A total of 14 peptides, covering the total length of the MSP-4 protein and peptide 34668 (²¹³GCGDDKLCEYVGNRRVKCKCK²³³), which was synthesized for correlating it with HABPs from other proteins that also display an EGF-like domain (MSP-1, -8, and -10), and 18 peptides covering the total length of MSP-7 were synthesized, purified, characterized, and tested in human erythrocyte receptor–ligand binding assays to determine whether MSP-4 and MSP-7 amino acid sequences were involved in specifically recognizing human erythrocyte surface molecules in the same way as other *P. falciparum* MSPs.

Only one HABP was found in the MSP-4 protein; peptide 20494 (²²¹EYVGNRRVKCKCKEGYKLEG²⁴⁰) was located in

the protein's carboxy-terminal region in the EGF-like domain.

Five HABPs were found in the MSP-7 protein: HABP 26101 (⁴¹IKNKKLEKLKNIVSGDFVGN⁶⁰) was located in the protein's N-terminal region, 26107 (¹⁶¹NLGLFGKNVLSKVKAQSETDY¹⁸⁰) was located in the central region, and 26114 (³⁰¹EKDKEYHEQFKNYIYGVYSYA³²⁰), 26115 (³²¹KQNSHLSEKKIKPEEEYK³⁴⁰), and 26116 (³³²EKPEEEYKFLSEYFNLLNTM³⁵¹) were located in the fragment's C-terminal region. The localization of HABPs 26101 and 26107 corresponded, respectively, to the 20 kDa fragment's N- and C-terminal extremes. HABPs 26114, 26115, and 26116 location corresponded to the 19 kDa fragment's C-terminal end (Figure 1b).

Human Erythrocyte HABP Binding Constants. Saturation binding assays were performed to determine the binding constants for human RBC interaction with HABPs. Saturation curve analysis showed that MSP-4 20494 and MSP-7 26101, 26107, and 26116 presented 470, 550, 600, and 450 nM dissociation constants, respectively. MSP-7 peptides 26114 and 26115 were not saturated in the working conditions used here. Calculations showed that there were around 24,000 binding sites per cell for MSP-4 HABPs 20494 and 70 000 to 145 000 binding sites per cell for MSP-7 26101, 26107, and 26116. Hill coefficients were higher than one, suggesting positive cooperativity (Figure 2 shows saturation curves and Hill plot).

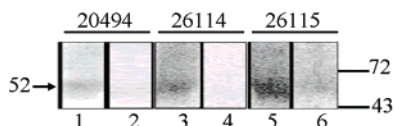


Figure 3. Cross-linking assays. Autoradiographs were obtained from human erythrocyte HABPs after binding had been cross-linked with ^{125}I -peptide 20494 of MSP-4 and ^{125}I -peptides 26114 and 26115 of MSP-7. Lanes 1, 3, and 5 show total binding (cross-linking in the absence of unlabeled peptide) and lanes 2, 4, and 6 show inhibited binding (cross-linking in the presence of unlabeled peptide). This figure shows that one possible receptor protein (52 kDa) is the same for all HABPs.

Table 1. MSP-4 and MSP-7 HABP Binding to Enzyme-Treated Human Erythrocytes^a

protein	peptide	neuraminidase	trypsin	chymotrypsin	control ^b (%)
MSP-4	20494	73 ± 5	57 ± 4	133 ± 9	100 ± 5
	26101	105 ± 7	174 ± 9	223 ± 10	100 ± 7
	26107	105 ± 7	0 ± 2	160 ± 9	100 ± 4
MSP-7	26114	73 ± 6	0 ± 3	34 ± 2	100 ± 6
	26115	57 ± 4	88 ± 3	73 ± 5	100 ± 6
	26116	100 ± 7	10 ± 1	0 ± 2	100 ± 4

^a Mean ± SD from three experiments. ^b Binding to normal erythrocytes was considered to be 100%.

HABP binding constants for MSP-4 20494 contained in the EGF-like domain I (determined in this study) and MSP-10 31132 contained in the EGF-like domain I⁴⁰ were very similar (Hill coefficient and K_d). The number of binding sites per cell was in the same order of magnitude, suggesting that these peptides could have been binding to the same, similar, or close erythrocyte surface receptors.

Cross-Linking Assays. Cross-linking assays showed that MSP-4 HABP 20494 and MSP-7 HABPs 26114, 26115, and 26116 bound to a 52 kDa molecule located on human RBC membrane. Figure 3 shows that HABP binding was specific and that ^{125}I -peptide binding was inhibited by nonradiolabeled peptide (i.e., radiolabeled peptide interaction with this protein was inhibited when the binding was performed in the presence of unlabeled peptide, indicating that it was a specific interaction). MSP-7 HABP 26116 showed less intensity in the 52 kDa band (data not shown).

Binding to Enzyme-Treated Erythrocytes. HABP binding was performed with enzyme-treated human RBC to determine each enzyme's effect on HABP interaction with human RBC surface. Nontreated human erythrocytes were used as positive control (Table 1). MSP-4-derived HABP 20494 binding was moderate when human RBC were treated with neuraminidase (~30%) and higher when treated with trypsin (~50%), suggesting that the receptor is probably associated with glycophorin A⁴². MSP-7-derived HABP 26101 binding to RBC was not susceptible to any of the enzymes used here. MSP-7-derived 26114 and 26116 were very susceptible to trypsin and chymotrypsin, suggesting that the receptor was probably band 3, while 26107 binding to RBCs was highly susceptible to just trypsin treatment, suggesting that the receptor was probably the putative "X" receptor.⁴²

Results observed for MSP-4 HABP 20494 were very similar to those presented recently for MSP-10 HABP 31132,⁴⁰ suggesting that peptides containing the EGF-like domain in their sequence bound to the same or similar erythrocyte receptor, as the binding of these HABPs was similarly affected by treatment with the same enzymes.

Merozoite Invasion Inhibition Assay. The possible role of MSP-4 and MSP-7 HABPs during merozoite invasion of human RBC was evaluated in *P. falciparum* inhibition assays performed

Table 2. Inhibition of Merozoite Invasion of Human Erythrocytes

protein	binding activity	peptide	invasion inhibition ^a (%)	
			200 μM	100 μM
MSP-4	high	20494	20 ± 2	16 ± 3
		34668	18 ± 2	3 ± 1
	low	20485	11 ± 2	9 ± 1
		high	26101	68 ± 2
MSP-7	high	26107	59 ± 1	9 ± 1
		26114	24 ± 3	7 ± 1
		26115	83 ± 3	22 ± 1
	low	26116	49 ± 0	9 ± 4
		26103	29 ± 3	10 ± 1
		chloroquine (0.5 mg/mL)		100 ± 3
EGTA (50 mM)		83 ± 3		

^a Mean ± SD from three experiments.

in vitro. These peptides were added to cultures at the schizont stage, before merozoites were released from infected erythrocytes. Results for the MSP-4 protein revealed that HABPs 20494 and 34668 inhibited invasion of RBC by ~20% at 200 μM concentration, while low-binding peptide 20485 inhibited invasion by ~10% at the same concentration. Results for MSP-7 protein HABPs showed that invasion was inhibited by more than 50% for HABPs 26101, 26107, 26115, and 26116 at 200 μM concentration, while low-binding peptide 26103 presented 20% invasion inhibition (Table 2). The assays were performed in triplicate; chloroquine and EGTA were used as positive controls and low-binding MSP-4 peptide 20485 and MSP-7 26103 were used as negative controls.

CD Spectroscopy. CD spectra were obtained in the presence of 30% TFE for determining HABP secondary structure. 26116-MSP-7 peptide's CD profile indicated a clearly ordered structure typical of an α -helix as characterized by double minima at 208, 220, and 190 nm maximum ellipticity (Figure 4, right-hand panel). The CD profiles for peptides 26101-MSP-7, 26107-MSP-7, 26114-MSP-7 (Figure 4, central panel), and 20494-MSP-4 (Figure 4, left-hand panel) had typical α -helix elements, while CD profiles for peptide 26115-MSP-7 corresponded to a completely random structure with a maximum ellipticity below zero and a minimum of around 200 nm (Figure 4, central panel). HABP 26115 (having random coil structure) had greater invasion inhibition activity; however, these results were not sufficient for establishing a direct structure–invasion inhibition activity relationship. Previous reports have shown that HABPs having an α -helical structure present similar or greater inhibition activity to HABPs having random coil structure.^{43,44}

Cross-Competition Assays. Binding competition assays were carried out between radiolabeled MSP-4 20494 peptide and the following nonradiolabeled autologous HABPs: MSP-4 20494, heterologous MSP-8 26373 and MSP-10 31132. MSP-4 34668 and MSP-4 20483 were used as control peptides. Figure 5 shows 45–75% radiolabeled peptide binding when competing with MSP-4 20494, MSP-10 31132, MSP-4 34668, and MSP-8 26373 peptides for greater nonradiolabeled peptide concentration. This experiment also showed that binding inhibition was concentration-dependent. Binding was 90–100% when competing with MSP-4 peptide 20483, which is not a HABP, thus not blocking MSP-4 20494 HABP binding to RBC.

Structural Analysis of MSP-1 19 kDa and Molecular Modeling Corresponding to MSP-10, MSP-8, and MSP-4 HABPs. Molecular modeling was done for comparing the different HABP locations in MSP-1, -4, -8, and -10 EGF-like domains. The *P. falciparum* MSP-1 19 kDa fragment (obtained by X-ray crystallography)^{39,43,44} consisted of amino acids presenting the following six β -sheets localized between residues

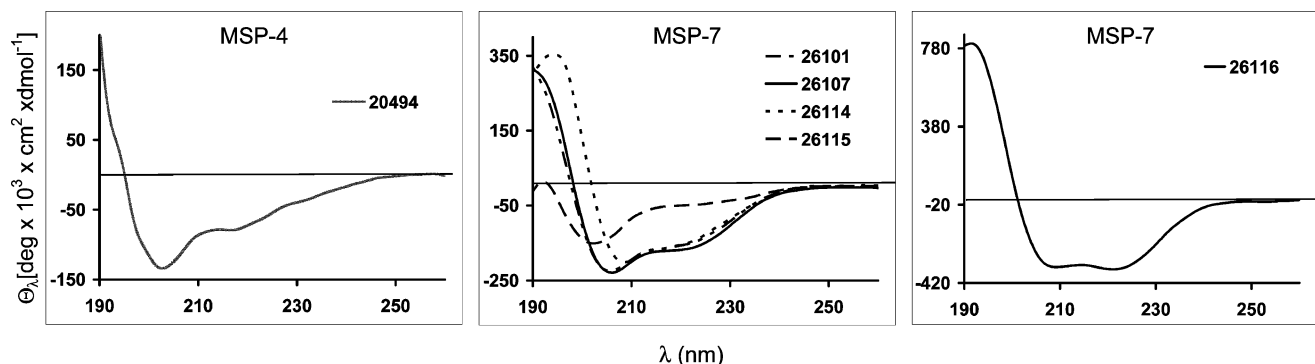


Figure 4. CD spectra. This figure shows graphs for HABP CDs. Peptide 26116-MSP7 displayed a curve characteristic of α -helix conformation (right-hand panel) and the same as MSP-4 HABP 20494 (left-hand panel), 26101, and 26107. MSP-7 26114 also showed a curve characteristic of α -helical elements.

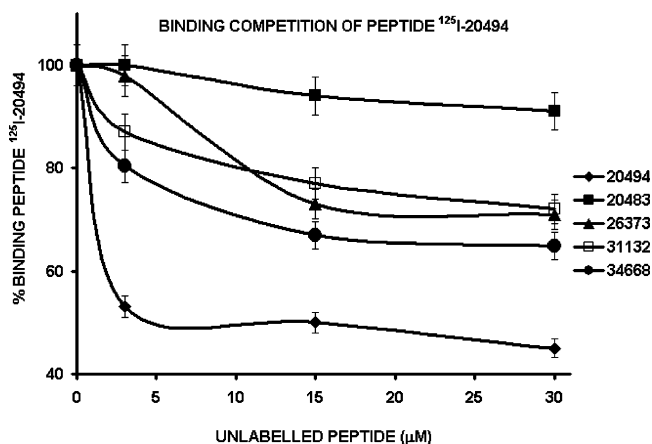


Figure 5. Binding competition of peptide ^{125}I -20494. Peptide 20494 was radiolabeled with ^{125}I and incubated with RBC in the presence of different concentrations of unlabelled peptide (MSP-4 20494, MSP-8 26373, MSP-10 31132, and MSP-4 34668 HABPs and low-binding MSP-4 20483 peptide).

16–21, 25–30, 34–36, 41–43, 61–63, and 75–77 and seven β -turns found between residues 3–6, 22–25, 31–34, 37–40, 49–53, 57–60, and 64–67. The disulfide bridges stabilizing the structure were Cys6 to Cys22, Cys7 to Cys18, Cys11 to Cys26, and Cys30 to Cys41 in the EGF-like domain I of this MSP-1 19 kDa fragment (Figure 6a,b). Because HABP 20494 is located in this EGF-like domain I, only these disulfide bridges have been taken into account in this manuscript.

The previously described MSP-1 19 kDa fragment HABP 5501 (running from Asn1 to Ser 16) presented a disulfide bridge between Cys7 and Cys18, having a β -turn between Ser3 and Gln6 residues. It was located entirely outside the structurally organized region of the EGF-like domain I (Figure 6c,d). RBC invasion was inhibited by $60 \pm 8\%$ at $200 \mu\text{M}$ by this peptide.³²

The MSP-10 19 kDa fragment was found between residues Cys1 to Asn85 and previously described HABP 31132 was located between Lys5–Cys24.⁴⁰ The disulfide bridge was formed in this HABP between Cys6 and Cys22. Predicting this HABP's structure (based on energy minimization and molecular modeling) suggested that this HABP had a β -turn structure between residues Ser7–Gln10 and two β -sheets between Ser10–Tyr13 and Gln21–Cys 24 residues (Figure 6c,d). RBC invasion was inhibited by $65 \pm 2\%$ at $200 \mu\text{M}$ by MSP-10 31132 HABP.⁴⁰

The MSP-8 19 kDa fragment was localized between Asn1–Ser87 residues; the also described MSP-8 HABP 26373 was

localized between Cys11–Cys30 and a disulfide bridge was formed between Cys11 and Cys26 (Figure 6c,d). This HABP has a totally random structure according to structure prediction. RBC invasion inhibition by HABP 26373 was $23 \pm 5\%$ at $200 \mu\text{M}$.³¹

The MSP-4 19 kDa fragment was located between Asn1 and Asn96 residues and HABP 20494 between Glu19 and Gly38. Disulfide bridges were found in this HABP between Cys12 and Cys28 and Cys 30 and Cys 41. Structural prediction studies suggested a β -turn from Val21–Arg24 residues and a β -sheet between Lys27–Cys30 and Gln21–Cys24 residues (Figure 6c,d). Inhibition of RBC invasion was $27 \pm 5\%$ at $200 \mu\text{M}$.

Alignment of MSP-1, -10, -8, and -4 HABPs Found in the 19 kDa Region. Based on amino acid sequence homologies and cysteine alignments of these GPI-anchored MSP HABPs, it was clearly seen in MSP-1 (5501), MSP-10 (31132), MSP-8 (26373), and MSP-4 (20494) HABP alignments (Figure 7) that when MSP-1 5501 HABP was used as a template, their RBC binding registers were displaced on the other HABPs by 6–18 residues toward these proteins' C-terminal end (e.g., MSP-1 5501 in relation to MSP-10 HABP 31132 displaced 10 residues upward and when compared to MSP-8 HABP 26373 displaced 11 residues). Likewise, MSP-4 HABP 20494 displaced six residues more toward the C-terminal end when compared to the MSP-8 26373 HABP and seven more when compared with MSP-10 31132. MSP-4 20494 displaced 18 residues backward regarding MSP-1 5501 HABP, suggesting a shift in these evolutionarily and functionally related MSP HABPs' GPI-anchored MSP 19 kDa fragments toward these molecules' C-terminal.

Discussion

Merozoite invasion of RBC occurs via several highly complex steps, which starts with merozoite rolling over the RBC membrane, reorientation toward the apical pole, penetration, parasitophorous vacuole (PV) formation,^{5,27,45} all involving receptor–ligand interactions between both host cell and parasite surface molecules.^{6–8,46}

It has been recently reported that several members of the MSP family (such as MSP-1 to MSP-10) are important in protein–protein interactions^{47,48} and forming lipid rafts on the merozoite membrane to mediate invasion of RBCs,⁴⁹ thus making them excellent targets for anti-malarial vaccine design.

Some MSP family members (MSP-1, -2, -4, -5, -8, and -10) contain the GPI motif,^{21,49} allowing them to remain anchored to the surface; other family members (MSP-3, -6, -7, and -9)

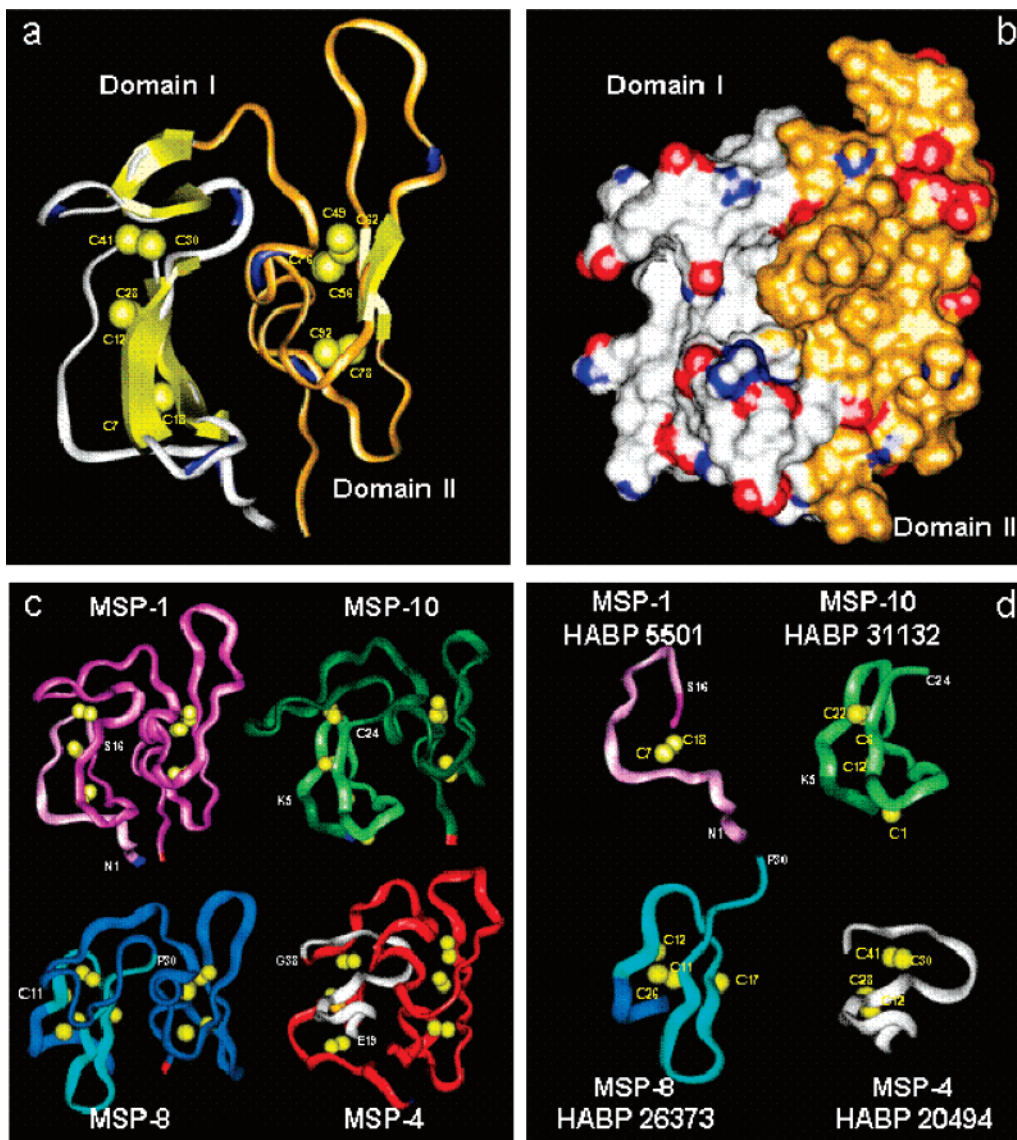


Figure 6. Three-dimensional (3D) structure. (a) MSP-1 19 kDa fragment calculations of the parallel, antiparallel sheet, and antiparallel turns were determined using DSSP program⁵⁸ and display the disulfide bridges (S atoms in yellow), the EGF-like domains I and II, as well as the unordered structures in both domains.³⁹ (b) Connolly representation of the MSP-1 19 kDa molecule structure; blue indicates positively charged atoms, red indicates negatively charged atoms, and white and golden colors are neutral residues. (c) 3D structure of the 19 kDa MSP-1 fragment in fuchsia,³⁹ and energy-minimization-based 3D structure predicted for the same homologous 19 kDa fragment in MSP-10 shown in green, MSP-8 shown in blue, and MSP-4 shown in red. The localization of MSP-1 HABP 5501 is shown in pink, MSP-10 31132 is shown in lemon green, MSP-8 26373 is shown in pale blue, and MSP-4 20494 is shown in white. (d) MSP-1 19 kDa 5501 HABP, as determined by NMR, and MSP-1 19 kDa-based prediction of the 3D structure of MSP-10 31132 HABP (lemon green), MSP-8 26373 HABP (pale blue), and MSP-4 20494 in white. Yellow balls correspond to cysteines determining EGF-like domains and establishing S–S bridges.

MSP-1 5501	1525 N I S Q H Q C V K K Q C P Q N S G C F R H L D E R E E C K C L L N Y K Q E G D K C 1565
MSP-10 31132	411 F K V N Y I C E Y S K C G P N S R C Y I V E K D K E Q C R C R P N Y I V D M S V N 451
MSP-8 26373	492 N N K V C E N T K - - C P L N S N C Y - V I D D E E T C R C L P G F N N I K I D D 529
MSP-4 20494	203 D E D L C K H N N G G C G D D K L C E Y V G N R R V K C K C K E G Y K L E G I E C 243

Figure 7. Alignments. Comparison of MSP-1, -10, -8, and -4 HABPs sequences.

are not directly bound to the membrane, but remain indirectly bound to it, being noncovalently associated with anchored proteins, such as MSP-1.^{23,49,50}

High specific binding regions or HABPs have been identified for several MSP family proteins, as well as their role in *P. falciparum* invasion of erythrocytes in in vitro assays.^{24,31,32,40} This work identifies and characterizes MSP-4 and MSP-7

proteins corresponding to HABPs in our endeavor to develop a logical and rational methodology for multi-epitope, multistage, subunit-based, chemically synthesized, antimalarial vaccine development.

Specific binding studies regarding MSP-4 synthetic peptide-derived protein interaction with human erythrocyte surface have shown that this protein interacts via its EGF-like domain I via

HABP 20494. This interaction's specificity was shown in saturation assays where a 470 nM dissociation constant was found, indicating that a small amount of peptide activated the receptor. Around 24 000 binding sites were found per cell (Figure 2).

Binding assays, using erythrocytes pretreated with different enzymes for MSP-4 HABP 20494, revealed that specific binding became reduced to a greater extent (~50%) when erythrocytes had been previously treated with trypsin, decreased to a lesser extent (~30) when treated with neuraminidase, whereas treatment with chymotrypsin did not reduce binding. These results suggested that the HABP 20494 receptor could be associated with glycophorin A or C; however, further studies are needed for elucidating the nature of such interaction with erythrocyte surface.

MSP-4 protein cross-linking assays showed that HABP 20494 had specific binding to a 52 kDa membrane protein (Figure 3), probably the dimer form of one of these glycophorins.

Binding competition assays revealed that the binding of radiolabeled peptide MSP-4 20494 HABP was concentration-dependent, regarding nonradiolabeled peptide 20494. Binding was inhibited by 50% at 30 μ M nonradiolabeled peptide 20494. Inhibition remained around 50% when varying nonradiolabeled peptide concentration. MSP-4 peptide 34668 only achieved 60% binding at 30 μ M, while 75% binding was achieved with MSP-10 peptide 31132 at 30 μ M and 78% with MSP-8 peptide 26373 at 30 μ M. No inhibition was noted with MSP-4 peptide 20483 (which is not a HABP). These results reinforce the idea of conserved structure for HABPs contained in EGF-like domains, as well as showing that binding to RBC was not inhibited with peptides, which did not present this structure.

HABP 5501 was found in the N-terminal unordered or nonstructurally organized region of the EGF-like domain I of MSP-1 19 kDa fragment. MSP-10 peptide 31132 was also located in this MSP-10 N-terminal region.^{31,32,40} Interestingly, HABP 20494 was situated in the structurally organized EGF-like domain I of MSP-4, and HABP 26373 was also located in this structurally ordered EGF-like domain I of MSP-8.

This result suggested the importance of this domain's structure to governing biological functions, such as binding and invasion of RBCs supported by other studies showing the importance of forming the EGF-like domain in MSP-4 protein antigenicity.^{12,51}

The fact that MSP-1 5501 HABP was located 10 residues upstream from MSP-10 31132 HABP and 26373 MSP-8 HABP and that MSP-4 HABP 20494 was 6 residues downstream of the last two HABPs mentioned above and 18 residues downstream of 5501 MSP-1 HABP, suggest a new strategy maintained by the *P. falciparum* parasite using redundant highly homologous members from the same family displaying minimal structural changes to avoid the differences posed by the receptors or host genetic variability and immune response.

These differences have a great structural and functional impact because they displayed different RBC invasion inhibitory ability at the same concentration as MSP-1-derived 5501 HABP having a mainly random structure with only one β -turn, which was able to inhibit RBC invasion by $60 \pm 8\%$. This was quite similar to 31132 MSP-10-derived HABP, which only had one β -turn and one β -sheet, both of them located in the unordered or nonstructurally organized region of the EGF-like domain I, inhibiting merozoite invasion of RBC by $65 \pm 2\%$.

MSP-8 26373-derived HABP (entirely included in EGF-like domain I structurally ordered or organized region) only inhibited merozoite invasion of RBC by $23 \pm 5\%$. MSP-4-derived HABP (completely included in the same ordered EGF-like domain I,

six residues downstream and displaying one β -turn and one β -sheet) inhibited merozoite invasion by $20 \pm 2\%$.

Very interestingly, the two HABPs displaying the highest invasion inhibition activity (MSP-1 5501 and MSP-10 31132) have their disulfide bridges between Cys-7 and Cys-18 (5501) and Cys-6 and Cys-22 (31132), while those having low inhibitory activity have their disulfide bridges between the cysteine residues located further back in the structurally configured or ordered EGF-like domain I in such a way that MSP-8 26376 has the S-S bridge between Cys-11 and Cys-26 and MSP-4 20494 between Cys-12 and Cys-28.

The data clearly show that, despite the fact that all these peptides bound with high affinity to RBC, only those located in the N-terminal unordered region located between Cys-7 and Cys-18 and Cys-6 and Cys-22 were highly relevant in RBC invasion, stressing the importance of localization in these HABPs' functional activity and the structural configuration determined by these intracysteine domains.

This information, having great functional impact, also has tremendous implications on immunological responses against the MSP-1 19 kDa fragment. Monoclonal antibodies (MoAb) produced against the 19 kDa fragment, as has been elegantly shown by Anthony Holder's group, are able to block merozoite invasion of RBC (such as monoclonal antibody 12.8) and recognize MSP-1 19 kDa fragment residues 5-13 and 14-18. Moreover, MoAb 12.10, also blocking merozoite invasion of RBC, recognized 19 kDa fragment residues 5-7 and 15-18.⁵² All these residues are MSP-1 5501 HABP components. MoAb 1E1, interfering with the blocking of invasion by MoAbs 12.8 and 12.10, recognized parental MSP-1 42 kDa fragment -5 to -3 residues, prior to this fragment's cleavage site.⁵³ Another noninvasion-inhibitory MoAb2F10 was primarily bound to EGF-like domain II in residues 49-56 and 66-73.⁵²

All of this biological, immunological, and structural data, plus MSP 19 kDa fragment homology with some other members of the MSP family anchored to the merozoite's membrane, strongly suggests that the relevant MSP-1 and MSP-10 protein regions, directly involved in RBC binding and able to induce a protection-inducing immune response, were located in the N-terminal region of the EGF-like domain I. MSP-1 HABP 5501 and MSP-10 HABP 31132 (residues 5-24) were located between residues 1-24 of this N-terminal region.

These HABPs present a high ability to inhibit merozoite invasion of RBC (~65%), while MSP-8 HABPs 26373 (residues 11-30) and MSP-4 20494 (residues 19-38), presenting low RBC invasion inhibition ability (~20%), were found to be displaced toward the ordered or structurally organized segment located toward the C-terminal region's 19 kDa fragment. This data clearly and strongly suggest that a protective immune response should be mainly directed against HABPs localized in the N-terminal, unordered region of these MSP molecules, such as MSP-1 5501 and MSP-10 31132.

It has been reported that merozoites expose a multiprotein complex on their surface during invasion; this is composed of proteolytically processed, noncovalently associated products from different membrane-associated proteins. It has been suggested that these complexes or co-ligands are involved in evading the immune response or in merozoite invasion of erythrocytes.⁵⁴⁻⁵⁶

The foregoing suggested that a cooperative effect was presented during invasion between binding regions (or HABPs) derived from the different proteins forming the multiprotein complex. This could explain the low invasion inhibition activity of some HABPs; an individual HABP could have a lower effect

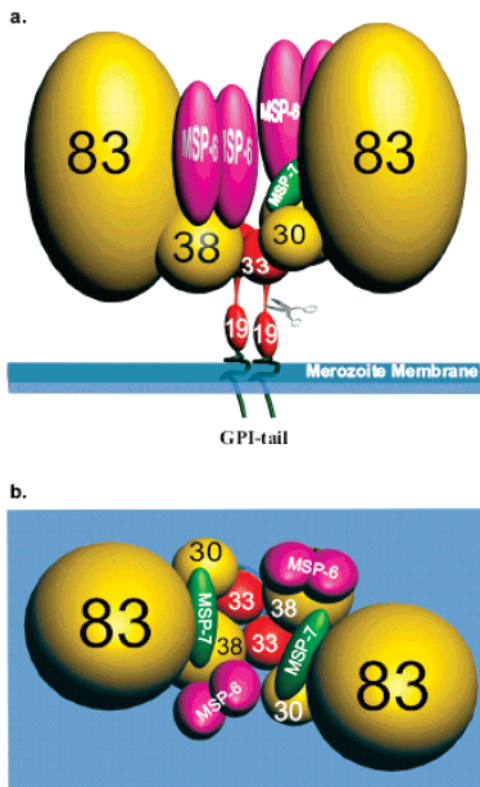


Figure 8. Graphic representation of merozoite surface proteins involved in RBC invasion forming macromolecular complexes. MSP-7 (green) molecules are noncovalently bound to noncovalently bound MSP-1 83 kDa, 30 kDa, and 38 kDa processed fractions but not to the 42 kDa fragment. This last fraction is further cleaved (scissors) into 33 kDa (red) and 19 kDa fragment (red), with the latter remaining anchored to the parasite's membrane via a GPI tail (black), this being the only MSP fraction carried into newly infected RBC. MSP-6 dimers (fuchsia) noncovalently bind exclusively to the MSP-1 38 kDa fragment: (a) front and (b) top views.

on inhibition compared to the inhibitory result of the whole protein or a group of HABPs.

All the above suggests that these MSP family members use their corresponding binding motifs' redundancy as immune response distractors or as alternative routes for invasion. This last phenomenon has been elegantly shown with erythrocyte binding ligand (EBL) and rhoptry (RhopH) proteins that when one of them (such as erythrocyte binding antigen 175 (EBA-175) is knocked-down or the receptor for this molecule on host cells is removed by enzymatic treatment or is not expressed, then the other proteins replace it during invasion, as happens between Rh-4 and EBA-175.⁵⁷

Regarding MSP-7, this mainly hydrophilic protein (33% charged residues) has a negative charge from residues 94 to 148.²² Specific studies of MSP-7 protein-derived synthetic peptides binding to human erythrocyte surface have suggested that this protein's interaction occurs via its C-terminal region, even though it also has HABPs in the N-terminal and intermediate regions. Previous studies have shown that this protein is cleaved and only the C-terminal region fragment is maintained;²³ this contained three of the five HABPs found, highlighting this region's importance.

MSP-7 HABPs 26114 and 26116 binding assays using erythrocytes pretreated with different enzymes have shown that specific binding has greater sensitivity when erythrocytes have been previously treated with trypsin and chymotrypsin, while binding was resistant to neuraminidase treatment. These results

suggested that these HABPs' receptor could have been associated with band 3 or "X" receptor.⁴²

Interestingly, MSP-4 HABP 20494 and MSP-7 HABPs 26114, 26115, and 26116 recognized an ~52 kDa protein on RBC membrane (Figure 3). It may have been that the HABPs bound to the same receptor at different binding sites; however, further studies are needed for determining the receptor's exact nature.

MSP7 protein HABPs' importance in invasion–inhibition assays should be stressed, as dependence on peptide concentration was noted (inhibiting invasion by 24–83% at 200 μ M concentration). HABP 26115 was able to inhibit merozoite invasion of RBC by up to 83%, once more suggesting this conserved region's importance following protein cleavage.

The most abundant complex at the merozoite surface to be shed is made up of MSP-1, 83 kDa, 30 kDa, and 38 kDa fragments, MSP-6 and MSP-7 (and probably some other proteins) that are noncovalently associated.

It has been clearly demonstrated that MSP-7 precursor interacts with MSP-1 83, 30, and 38 kDa fragments but not with 42 kDa or its corresponding 33 kDa and 19 kDa cleavage products (Figure 8a,b)⁴⁷ being a member of the proteins noncovalently bound to the merozoite membrane via binding to other membrane-anchored proteins like MSP-1 in detergent-resistant membrane (DRM) protein lipid rafts (Figure 8a,b).⁴⁹

While MSP-6 requires processing for binding to the previously assembled MSP-1 complex, MSP-7 precursor does not require processing and is capable of interaction with all but 42 kDa MSP-1 cleavage products, as established before.

Conclusions

MSP-4 and MSP-7 HABPs, as identified in this assay, are relevant in merozoite invasion of RBC, and structure–function correlations were found for some MSP members. This led to suggesting a new mechanism for explaining protein redundancy, thereby making them excellent new HABPs to be included in further studies for developing a subunit-based, multi-epitope, multistage, chemically produced, antimalarial vaccine, a goal our institute has been pursuing for the last three decades.

Acknowledgment. This work was financed by Colciencias Contract RC 041-2007. We would particularly like to thank Jason Garry for reviewing this manuscript.

References

- (1) Snow, R. W.; Guerra, C. A.; Noor, A. M.; Myint, H. Y.; Hay, S. I. The global distribution of clinical episodes of *Plasmodium falciparum* malaria. *Nature* **2005**, *434*, 214–217.
- (2) Miller, L. H.; Baruch, D. I.; Marsh, K.; Doubo, O. K. The pathogenic basis of malaria. *Nature* **2002**, *415*, 673–679.
- (3) Cowman, A. F.; Crabb, B. S. Invasion of red blood cells by malaria parasites. *Cell* **2006**, *124*, 755–766.
- (4) Dvorak, J. A.; Miller, L. H.; Whitehouse, W. C.; Shiroishi, T. Invasion of erythrocytes by malaria merozoites. *Science* **1975**, *187*, 748–750.
- (5) Aikawa, M.; Miller, L. H.; Johnson, J.; Rabbage, J. Erythrocyte entry by malarial parasites. A moving junction between erythrocyte and parasite. *J. Cell Biol.* **1978**, *77*, 72–82.
- (6) Chitnis, C. E. Molecular insights into receptors used by malaria parasites for erythrocyte invasion. *Curr. Opin. Hematol.* **2001**, *8*, 85–91.
- (7) Preisner, P.; Kaviratne, M.; Khan, S.; Bannister, L.; Jarra, W. The apical organelles of malaria merozoites: host cell selection, invasion, host immunity and immune evasion. *Microbes Infect.* **2000**, *2*, 1461–1477.
- (8) Bozdech, Z.; Llinás, M.; Pulliam, B. L.; Wong, E. D.; Zhu, J.; DeRisi, J. L. The transcriptome of the intraerythrocytic developmental cycle of *Plasmodium falciparum*. *PLoS Biol.* **2003**, *1*, E5.
- (9) Oeuvray, C.; Bouharoun-Tayoun, H.; Gras-Masse, H.; Bottius, E.; Kaidoh, T.; Aikawa, M.; Filgueira, M. C.; Tartar, A.; Druilhe, P. Merozoite surface protein-3: A malaria protein inducing antibodies that promote *Plasmodium falciparum* killing by cooperation with blood monocytes. *Blood* **1994**, *84*, 1594–1602.

- (10) Saul, A.; Lawrence, G.; Smillie, A.; Rzepczyk, C. M.; Reed, C.; Taylor, D.; Anderson, K.; Stowers, A.; Kemp, R.; Allworth, A.; Anders, R. F.; Brown, G. V.; Pye, D.; Schoofs, P.; Irving, D. O.; Dyer, S. L.; Woodrow, G. C.; Briggs, W. R. S.; Reber, R.; Sturchler, D. Human phase I vaccine trials of three recombinant asexual stage malaria antigens with Montanide ISA720 adjuvant. *Vaccine* **1999**, *17*, 3145–3159.
- (11) Stowers, A. W.; Cioce, V.; Shimp, R. L.; Lawson, M.; Hui, G.; Muratova, O.; Kaslow, D. C.; Robinson, R.; Long, C. A.; Miller, L. H. Efficacy of two alternate vaccines based on *Plasmodium falciparum* merozoite surface protein 1 in an Aotus challenge trial. *Infect. Immun.* **2001**, *69*, 1536–1546.
- (12) Wang, L.; Richie, T. L.; Stowers, A.; Nhan, D. H.; Coppel, R. L. Naturally acquired antibody responses to *Plasmodium falciparum* merozoite surface protein 4 in a population living in an area of endemicity in Vietnam. *Infect. Immun.* **2001**, *69*, 4390–4397.
- (13) Blackman, M. J.; Ling, I. T.; Nicholls, S. C.; Holder, A. A. Proteolytic processing of the *Plasmodium falciparum* merozoite surface protein-1 produces a membrane-bound fragment containing two epidermal growth factor-like domains. *Mol. Biochem. Parasitol.* **1991**, *49*, 29–33.
- (14) Holder, A. A.; Freeman, R. R. The three major antigens on the surface of *Plasmodium falciparum* merozoites are derived from a single high molecular weight precursor. *J. Exp. Med.* **1984**, *160*, 624–629.
- (15) Blackman, M. J.; Holder, A. A. Secondary processing of the *Plasmodium falciparum* merozoite surface protein-1 (MSP1) by a calcium-dependent membrane-bound serine protease: shedding of MSP133 as a noncovalently associated complex with other fragments of the MSP1. *Mol. Biochem. Parasitol.* **1992**, *50*, 307–315.
- (16) Blackman, M. J.; Whittle, H.; Holder, A. A. Processing of the *Plasmodium falciparum* major merozoite surface protein-1: Identification of a 33-kilodalton secondary processing product which is shed prior to erythrocyte invasion. *Mol. Biochem. Parasitol.* **1991**, *49*, 35–44.
- (17) Blackman, M. J.; Heidrich, H. G.; Donachie, S.; McBride, J. S.; Holder, A. A. A single fragment of a malaria merozoite surface protein remains on the parasite during red cell invasion and is the target of invasion-inhibiting antibodies. *J. Exp. Med.* **1990**, *172*, 379–382.
- (18) Egan, A. F.; Chappel, J. A.; Burghaus, P. A.; Morris, J. S.; McBride, J. S.; Holder, A. A.; Kaslow, D. C.; Riley, E. M. Serum antibodies from malaria-exposed people recognize conserved epitopes formed by the two epidermal growth factor motifs of MSP1(19), the carboxy-terminal fragment of the major merozoite surface protein of *Plasmodium falciparum*. *Infect. Immun.* **1995**, *63*, 456–466.
- (19) Egan, A. F.; Morris, J.; Barnish, G.; Allen, S.; Greenwood, B. M.; Kaslow, D. C.; Holder, A. A.; Riley, E. M. Clinical immunity to *Plasmodium falciparum* malaria is associated with serum antibodies to the 19-kDa C-terminal fragment of the merozoite surface antigen, PfMSP-1. *J. Infect. Dis.* **1996**, *173*, 765–769.
- (20) Marshall, V. M.; Silva, A.; Foley, M.; Cranmer, S.; Wang, L.; McColl, D. J.; Kemp, D. J.; Coppel, R. L. A second merozoite surface protein (MSP-4) of *Plasmodium falciparum* that contains an epidermal growth factor-like domain. *Infect. Immun.* **1997**, *65*, 4460–4467.
- (21) Gowda, D. C.; Gupta, P.; Davidson, E. A. Glycosylphosphatidylinositol anchors represent the major carbohydrate modification in proteins of intraerythrocytic stage *Plasmodium falciparum*. *J. Biol. Chem.* **1997**, *272*, 6428–6439.
- (22) Pachebat, J. A.; Ling, I. T.; Grainger, M.; Trucco, C.; Howell, S.; Fernandez-Reyes, D.; Gunaratne, R.; Holder, A. A. The 22 kDa component of the protein complex on the surface of *Plasmodium falciparum* merozoites is derived from a larger precursor, merozoite surface protein 7. *Mol. Biochem. Parasitol.* **2001**, *117*, 83–89.
- (23) Pachebat, J. A.; Kadekoppala, M.; Grainger, M.; Dluzewski, A. R.; Gunaratne, R. S.; Scott-Finnigan, T. J.; Ogun, S. A.; Ling, I. T.; Bannister, L. H.; Taylor, H. M.; Mitchell, G. H.; Holder, A. A. Extensive proteolytic processing of the malaria parasite merozoite surface protein 7 during biosynthesis and parasite release from erythrocytes. *Mol. Biochem. Parasitol.* **2007**, *151*, 59–69.
- (24) Lopez, R.; Valbuena, J.; Rodriguez, L. E.; Ocampo, M.; Vera, R.; Curtidor, H.; Puentes, A.; Garcia, J.; Ramirez, L. E.; Patarroyo, M. E. *Plasmodium falciparum* merozoite surface protein 6 (MSP-6) derived peptides bind erythrocytes and partially inhibit parasite invasion. *Peptides* **2006**, *27*, 1685–1692.
- (25) Ocampo, M.; Vera, R.; Rodriguez, L. E.; Curtidor, H.; Suarez, J.; Garcia, J.; Puentes, A.; Lopez, R.; Valbuena, J.; Tovar, D.; Reyes, C.; Vega, S.; Patarroyo, M. E. Identification of *Plasmodium falciparum* reticulocyte binding protein RBP-2 homologue a and b (PIRBP-2-Ha and -Hb) sequences that specifically bind to erythrocytes. *Parasitol. Int.* **2004**, *53*, 77–88.
- (26) Rodriguez, L. E.; Urquiza, M.; Ocampo, M.; Curtidor, H.; Suarez, J.; Garcia, J.; Vera, R.; Puentes, A.; Lopez, R.; Pinto, M.; Rivera, Z.; Patarroyo, M. E. *Plasmodium vivax* MSP-1 peptides have high specific binding activity to human reticulocytes. *Vaccine* **2002**, *20*, 1331–1339.
- (27) Cowman, A. F.; Baldi, D. L.; Healer, J.; Mills, K. E.; O'Donnell, R. A.; Reed, M. B.; Triglia, T.; Wickham, M. E.; Crabb, B. S. Functional analysis of proteins involved in *Plasmodium falciparum* merozoite invasion of red blood cells. *FEBS Lett.* **2000**, *476*, 84–88.
- (28) Goschnick, M. W.; Black, C. G.; Kedzierski, L.; Holder, A. A.; Coppel, R. L. Merozoite surface protein 4/5 provides protection against lethal challenge with a heterologous malaria parasite strain. *Infect. Immun.* **2004**, *72*, 5840–5849.
- (29) Houghten, R. A. General method for the rapid solid-phase synthesis of large numbers of peptides: specificity of antigen-antibody interaction at the level of individual amino acids. *Proc. Natl. Acad. Sci. U.S.A.* **1985**, *82*, 5131–5135.
- (30) Curtidor, H.; Ocampo, M.; Rodriguez, L. E.; Lopez, R.; Garcia, J. E.; Valbuena, J.; Vera, R.; Puentes, A.; Leiton, J.; Cortes, L. J.; Lopez, Y.; Patarroyo, M. A.; Patarroyo, M. E. *Plasmodium falciparum* TryThrA antigen synthetic peptides block in vitro merozoite invasion to erythrocytes. *Biochem. Biophys. Res. Commun.* **2006**, *339*, 888–896.
- (31) Puentes, A.; Garcia, J.; Ocampo, M.; Rodriguez, L.; Vera, R.; Curtidor, H.; Lopez, R.; Suarez, J.; Valbuena, J.; Vanegas, M.; Guzman, F.; Tovar, D.; Patarroyo, M. E. *P. falciparum* Merozoite surface protein-8 peptides bind specifically to human erythrocytes. *Peptides* **2003**, *24*, 1015–1023.
- (32) Urquiza, M.; Rodriguez, L. E.; Suarez, J. E.; Guzmán, F.; Ocampo, M.; Curtidor, H.; Segura, C.; Trujillo, E.; Patarroyo, M. E. Identification of *Plasmodium falciparum* MSP-1 peptides able to bind to human red blood cells. *Parasite Immunol.* **1996**, *18*, 515–526.
- (33) García, J. E.; Puentes, A.; López, R.; Vera, R.; Suárez, J.; Rodríguez, L.; Curtidor, H.; Ocampo, M.; Tovar, D.; Forero, M.; Bermudez, A.; Cortés, J.; Urquiza, M.; Patarroyo, M. E. Peptides of the liver stage antigen-1 (LSA-1) of *Plasmodium falciparum* bind to human hepatocytes. *Peptides* **2003**, *24*, 647–657.
- (34) Lambros, C.; Vanderberg, J. P. Synchronization of *Plasmodium falciparum* erythrocytic stages in culture. *J. Parasitol.* **1979**, *65*, 418–420.
- (35) Wyatt, C. R.; Goff, W.; Davis, W. C. A flow cytometric method for assessing viability of intraerythrocytic hemoparasites. *J. Immunol. Methods* **1991**, *140*, 23–30.
- (36) Provencher, S. W.; Glöckner, J. Estimation of globular protein secondary structure from circular dichroism. *Biochemistry* **1981**, *20*, 33–37.
- (37) Higgins, D. G.; Sharp, P. M. CLUSTAL: A package for performing multiple sequence alignment on a microcomputer. *Gene* **1988**, *73*, 237–244.
- (38) Combet, C.; Jambon, M.; Deléage, G. Geno3D: Automatic comparative molecular modelling of protein. *Bioinformatics* **2002**, *18*, 213–214.
- (39) Morgan, W. D.; Birdsall, B.; Frenkiel, T. A.; Gradwell, M. G.; Burghaus, P. A.; Syed, S. E. H.; Uthaipibull, C.; Holder, A. A.; Feeney, J. Solution structure of an EGF module pair from the *Plasmodium falciparum* merozoite surface protein 1. *J. Mol. Biol.* **1999**, *289*, 113–122.
- (40) Puentes, A.; Ocampo, M.; Rodriguez, L. E.; Vera, R.; Valbuena, J.; Curtidor, H.; Garcia, J.; Lopez, R.; Tovar, D.; Cortes, J.; Rivera, Z.; Elkin Patarroyo, M. Identifying *Plasmodium falciparum* merozoite surface protein-10 human erythrocyte specific binding regions. *Biochimie* **2005**, *87*, 461–472.
- (41) Laskowski, R. A.; Rullmann, J. A.; MacArthur, M. W.; Kaptein, R.; Thornton, J. M. AQUA and PROCHECK-NMR: Programs for checking the quality of protein structures solved by NMR. *J. Biomol. NMR* **1996**, *8*, 477–486.
- (42) Baum, J.; Maier, A. G.; Good, R. T.; Simpson, K. M.; Cowman, A. F. Invasion by *P. falciparum* merozoites suggests a hierarchy of molecular interactions. *PLoS Pathog.* **2005**, *1*, e37.
- (43) Chitarra, V.; Holm, I.; Bentley, G. A.; Pétres, S.; Longacre, S. The crystal structure of C-terminal merozoite surface protein 1 at 1.8 Å resolution, a highly protective malaria vaccine candidate. *Mol. Cell* **1999**, *3*, 457–464.
- (44) Pizarro, J. C.; Chitarra, V.; Verger, D.; Holm, I.; Petres, S.; Dartevelle, S.; Nato, F.; Longacre, S.; Bentley, G. A. Crystal structure of a Fab complex formed with PfMSP1-19, the C-terminal fragment of merozoite surface protein 1 from *Plasmodium falciparum*: A malaria vaccine candidate. *J. Mol. Biol.* **2003**, *328*, 1091–1103.
- (45) Hadley, T. J. Invasion of erythrocytes by malaria parasites: A cellular and molecular overview. *Annu. Rev. Microbiol.* **1986**, *40*, 451–477.

- (46) Cowman, A. F.; Crabb, B. S. The *Plasmodium falciparum* genome—a blueprint for erythrocyte invasion. *Science* **2002**, *298*, 126–128.
- (47) Kauth, C. W.; Woehlbier, U.; Kern, M.; Mekonnen, Z.; Lutz, R.; Mücke, N.; Langowski, J.; Bujard, H. Interactions between merozoite surface proteins 1, 6, and 7 of the malaria parasite *Plasmodium falciparum*. *J. Biol. Chem.* **2006**, *281*, 31517–31527.
- (48) Li, X.; Chen, H.; Oo, T. H.; Daly, T. M.; Bergman, L. W.; Liu, S. C.; Chishti, A. H.; Oh, S. S. A co-ligand complex anchors *Plasmodium falciparum* merozoites to the erythrocyte invasion receptor band 3. *J. Biol. Chem.* **2004**, *279*, 5765–5771.
- (49) Sanders, P. R.; Gilson, P. R.; Cantin, G. T.; Greenbaum, D. C.; Nebl, T.; Carucci, D. J.; McConville, M. J.; Schofield, L.; Hodder, A. N.; Yates, J. R.; Crabb, B. S. Distinct protein classes including novel merozoite surface antigens in Raft-like membranes of *Plasmodium falciparum*. *J. Biol. Chem.* **2005**, *280*, 40169–40176.
- (50) Trucco, C.; Fernandez-Reyes, D.; Howell, S.; Stafford, W. H.; Scott-Finnigan, T. J.; Grainger, M.; Ogun, S. A.; Taylor, W. R.; Holder, A. A. The merozoite surface protein 6 gene codes for a 36 kDa protein associated with the *Plasmodium falciparum* merozoite surface protein-1 complex. *Mol. Biochem. Parasitol.* **2001**, *112*, 91–101.
- (51) Wang, L.; Black, C. G.; Marshall, V. M.; RL., C. Structural and antigenic properties of merozoite surface protein 4 of *Plasmodium falciparum*. *Infect. Immun.* **1999**, *67*, 2193–2200.
- (52) Morgan, W. D.; Lock, M. J.; Frenkiel, T. A.; Grainger, M.; Holder, A. A. Malaria parasite-inhibitory antibody epitopes on *Plasmodium falciparum* merozoite surface protein-119 mapped by TROSY NMR. *Mol. Biochem. Parasitol.* **2004**, *138*, 29–36.
- (53) Uthaiyibull, C.; Aufiero, B.; Syed, S. E. H.; Hansen, B.; Patino, J. A. G.; Angov, E.; Ling, I. T.; Fegeding, K.; Morgan, W. D.; Ockenhouse, C.; Birdsall, B.; Feeney, J.; Lyon, J. A.; Holder, A. A. Inhibitory and blocking monoclonal antibody epitopes on merozoite surface protein 1 of the malaria parasite *Plasmodium falciparum*. *J. Mol. Biol.* **2001**, *307*, 1381–1394.
- (54) Kariuki, M. M.; Li, X.; Yamodo, I.; Chishti, A. H.; Oh, S. S. Two *Plasmodium falciparum* merozoite proteins binding to erythrocyte band 3 form a direct complex. *Biochem. Biophys. Res. Commun.* **2005**, *338*, 1690–1695.
- (55) Kauth, C. W.; Woehlbier, U.; Kern, M.; Mekonnen, Z.; Lutz, R.; Mücke, N.; Langowski, J.; Bujard, H. Interactions between merozoite surface proteins 1, 6, and 7 of the malaria parasite *Plasmodium falciparum*. *J. Biol. Chem.* **2006**, *281*, 31517–31527.
- (56) Sanders, P. R.; Gilson, P. R.; Cantin, G. T.; Greenbaum, D. C.; Nebl, T.; Carucci, D. J.; McConville, M. J.; Schofield, L.; Hodder, A. N.; Yates, J. R., 3rd; Crabb, B. S. Distinct protein classes including novel merozoite surface antigens in Raft-like membranes of *Plasmodium falciparum*. *J. Biol. Chem.* **2005**, *280*, 40169–76.
- (57) Stubbs, J.; Simpson, K. M.; Triglia, T.; Plouffe, D.; Tonkin, C. J.; Duraisingh, M. T.; Maier, A. G.; Winzeler, E. A.; Cowman, A. F. Molecular mechanism for switching of *P. falciparum* invasion pathways into human erythrocytes. *Science* **2005**, *309*, 1384–1387.
- (58) Kabsch, W.; Sander, C. How good are predictions of protein secondary structure? *FEBS Lett.* **1983**, *155*, 179–182.

JM070773Z